Original Article

Interactive Effects of Endothelial Colony-Forming Cells with Adipose Mesenchymal Stem Cells on the Pancreas of Type 2 Diabetic Rat Model: A Histological Study

Marwa Mohamed Yousry and Eman Abas Farag

Department of Histology, Faculty of Medicine, Cairo University, Cairo, Egypt

ABSTRACT

Background: Adipose mesenchymal stem cells (AMSCs) appeared as a promising therapy for type 2 diabetes (T2D). However, single AMSCs infusion could be insufficient to exert sustained antidiabetic effects. Endothelial colony forming cells (ECFCs) are implicated in various biologic processes as vascular homeostasis, neovascularization and tissue regeneration.

Aim of Work: Assessing and comparing the reparative effect of AMSCs on induced T2D rats at different time points with the potential effect of cotherapy with ECFCs.

Materials and Methods: Four rats of a total sixty adult male albino rats were used for AMSCs and ECFCs preparation and labelling with PKH26. Animals were divided into 4 main groups: I (control), II (T2D); received high fat diet for 5 weeks then received single intraperitoneal injection of STZ (40mg/kg) and continued HFD for one week. Group III (AMSCs treated) diabetic rats administered AMSCs and group IV (combined, AMSCs +ECFCs) diabetic rats received AMSCs+ECFCs. One rat from groups III and IV with their corresponded control were sacrificed 1 week after cells injection to assess homing at pancreatic tissue and the remaining rats were sacrificed after 2&6 weeks. Biochemical analysis and histological studies including H&E stain, insulin, caspase-3, CD146, Sox9 immunohistochemical stains & TEM were done followed by morphometric measurements and statistical analysis.

Results: T2D rats revealed biochemical and histological derangement in islets' β cells and vascularity with areas of stratification in pancreatic ducts. Rats treated with AMSCs only or combined with ECFCs revealed improved insulin sensitivity, glucose homeostasis and nearly normal histological features after 2 weeks. After 6 weeks biochemical and histological ameliorations regressed in AMSCs treated rats. On the contrary, cotherapy of AMSCs +ECFCs extended this anti-diabetic effect.

Conclusion: ECFCs cotherapy with AMSCs prolonged and enhanced the anti-diabetic effect of AMSCs in T2D by enhancement of islets cells regeneration, islets vasculature, and probably by duct epithelium trans-differentiation.

Received: 08 February 2022, **Accepted:** 13 February 2022

Key Words: AMSCs+ ECFCs, CD146, insulin, pericytes, Sox9, T2D.

Corresponding Author: Marwa Mohamed Yousry, MD, Department of Histology, Faculty of Medicine, Cairo University, Cairo, Egypt, **Tel.**: +20 10 0676 3862, **E-mail:** marwa.yousry@cu.edu.eg

ISSN: 1110-0559, Vol. 46, No. 2

BACKGROUND

Type 2 diabetes (T2D) is one of the most common forms of chronic disease. Global prevalence of T2D is predicted to increase to 7079 individuals per 100,000 by 2030, mirroring a continued increase across all regions of the world[1]. T2D which accounts for 90–95% of all diabetes, is essentially characterized by pancreatic β-cell dysfunction and insulin resistance[2] and associated by disorders of glucose and lipid metabolism[3]. These disorders are the basic pathology causing microvascular and macrovascular complications[4]. The pancreatic islet, a complex network of multiple cell types, contains the central regulator of glucose homeostasis mainly beta (β) and alpha (α) cells, as well as non-endocrine cell types comprising sympathetic and parasympathetic nerves and an extended capillary network including endothelial cells (ECs) and supportive cells such as pericytes[5]. The integrated action of all these cell types is needed for proper islet function. Based on that, several researchers clarified that the pathogenesis of T2D is associated with dysfunction of the pancreatic islet cells and its vasculature[6].

Consequently, the alterations in islet endothelial cell function and morphology might represent an important contributor to impaired survival of β cell and insulin secretory function in T2D[7].

So far, the available therapeutic regimens target either insulin resistance or insulin deficiency[8]. Excellent metabolic control without the use of exogenous insulin can be accomplished with transplantation of whole pancreas or islet cells. However, this procedure is very limited due to the immunological risks that affect long-term survival[9]. Therefore, regeneration of the endogenous β-cells via stem cells is now considered as the perfect curative tool[10].

Mesenchymal stem cells (MSCs) are one of the most significant multipotent adult stem cells that can be derived from multiple sources such as bone marrow, cord blood, or adipose tissue. In comparison with the bone marrow mesenchymal stem cells (BM-MSCs), adipose mesenchymal stem cells (AMSCs) offer numerous advantages; large number of cells can be easily collected by liposuction; expansion and differentiation of cells

 DOI: 10.21608/ejh.2022.120852.1641

are easier[11] and have around threefold increase in immunosuppressive activity[12].

Unfortunately, the beneficial response to a single MSCs infusion in both diabetic animal models and patients usually occurs immediately and is maintained for a limited time[13,14]. This relatively temporary role had led many researchers to explore effective approaches to strengthen or prolong the antidiabetic effects of MSCs[15].

Endothelial colony-forming cells (ECFCs), a subset of endothelial progenitor cells (EPCs), can be isolated from human cord or peripheral blood and have robust clonal proliferative potential[16]. ECFCs possessed potent intrinsic angiogenic effect through contribution of vascular repair and de novo blood vessel formation[17]. However, in *vitro* ECFCs of diabetic patients appeared compromised compared to healthy controls with defective mobilization, migration, proliferation and poor vascular endothelial repair[18]. Therefore, the present study aimed at assessing and comparing the amending effect of AMSCs injection on experimental T2D rats at different time points and the potential role of ECFCs cotherapy.

MATERIALS AND METHODS

Experimental Design

Sixty adult male albino rats with an average body weight of 200g were treated according to Cairo University Animal Use Committee guidelines (CU-III-F-13-21). The rats were housed in The Laboratory Animal House Unit of Kasr Al-Aini, Faculty of Medicine, Cairo University and were subjected to a normal light/dark cycle and allowed free access to chow and water.

One week after acclimatization, four rats were used for adipose tissue MSCs (AMSCs) and endothelial colony forming cells (ECFCs) isolation, culture, phenotyping, and labelling. The remaining animals were divided randomly into 4 main groups (I, II, III &IV).

Group I (Control Group) (18 rats): The animals were provided with ordinary rat chow with free water and food access and were divided into four subgroups:

- Subgroup Ia (4 rats): received no treatment.
- Subgroup Ib (4 rats): after 5 weeks from the beginning of the experiment, rats were received single intraperitoneal (IP) injection of 0.25ml citrate buffer saline after being fasted overnight and maintained for one week on ordinary rat chow.
- Subgroup Ic (5 rats): prepared as subgroup Ib then the rats were given 0.2ml of PKH26 labelled AMSCs suspension in PBS (1×10^6 cells/ 0.2ml) once through the tail vein.
- Subgroup Id (5 rats): prepared similar to subgroup Ic but they were additionally coinjected, at the same time, with PKH26 labelled ECFCs (1×10^5 cells/ 0.2ml) through the tail vein.

Group II (T2D) (12 rats): Type 2 diabetes was induced, according to previous study[19] by administration of high fat diet (HFD) (Teklad Adjusted Fat Diet, TD #96132; Harlan, Envigo laboratory animal diets). This diet expressed nearly as a percentage of weight content as follows: 40% fat, 41% carbohydrate and 18% protein) for 5 weeks. Then the rats were fasted overnight and injected IP with 0.25ml of a single freshly prepared streptozotocin (STZ) purchased from Sigma Company (St. Louis, MO, USA) at a dose of (40mg/kg) dissolved in 0.1 M/L citrate buffer saline, pH =4.5. The STZ treated rats continued on HFD for one week. Following the total period of diabetes induction, 6 weeks, diabetes was considered when fasting blood glucose level was above 16.7 mmol/L.

Group III (AMSCs treated): (13rats): diabetes was induced similar to group II and then after diabetes confirmation the rats received single injection of 0.2ml PBS containing 1×10^6 PKH26 labelled AMSCs through the tail vein[8].

Group IV (combined or cotherapy group) (AMSCs+ECFCs): (13rats): diabetic animals were treated as group III, but they were also injected, following diabetes confirmation, with PKH26 labelled ECFCs (1×10^5 cells/ 0.2ml PBS) once through the tail vein[20].

One rat from groups III and IV and their corresponded control subgroups Ic and Id respectively were sacrificed after one week of cellular injection for detection of AMSCs and ECFCs homing then the remaining animals of all groups were equally subdivided into 2 subgroups (2W&6W) respective to sacrifice at 2 & 6 weeks following diabetes confirmation.

In Vitro Studies

PKH26 labelled AMSCs and ECFCs were purchased from stem cell research unit at the Biochemistry Department, Faculty of Medicine, Cairo University.

Preparation of AMSCs

Under complete aseptic conditions, the subcutaneous white adipose tissue was excised from rat's inguinal pad of fat. Then the excised tissue was placed into a labelled sterile tube containing 15 ml of a PBS (Sigma, USA, P5493) and was subjected to previously described methodology[21] until the first-passage culture was created which then expanded in *vitro* until 4th passage. Cultured AMSCs were morphologically identified as previously described by their adhesiveness, fusiform shape and by flow cytometry detection of CD29, one of the surface markers of rat AMSCs[22]. Differentiation of AMSCs into chondrocytes and osteocytes using cell differentiation kits according to the manufacturer's recommendation (Mo Bi Tec., Lorzestrasse, Germany) was confirmed[23].

Preparation of ECFCs

ECFCs were obtained from peripheral blood as former methodology[24] and the resultant ECFCs colonies were 80%. Then the ECFCs were cultured in Endothelial Basal Medium MV2 (PromoCell) and used between passages

2–5[25]. The ECFCs were phenotypically characterized as previously described and appeared as spindle shaped cells with cobblestone morphology[26].

Labelling of AMSCs and ECFCs

AMSCs and ECFCs were labelled using Red PKH26 Fluorescent Cell Linker Kit (Sigma, USA, MINI26) according to the manufacturer's protocol.

Animal Studies

Biochemical Analysis

After diabetes induction, blood samples were withdrawn from tail veins of all animals in animal house then biochemical analysis was done at Biochemistry Department, Faculty of Medicine, Cairo University at the end of week 2 &6 for monitoring of:

- Fasting blood glucose level (FBG): was assessed using reagent kits purchased from Bio Merieux Chemicals (France).
- Fasting insulin level (FINS): was measured by enzyme immunoassay using the rat insulin ELISA kits (Linco research).
- Glycosylated hemoglobin (GHb) percent: GHb is a product of non-enzyme glycosylation and considered as a principle parameter for monitoring the control of diabetes and assessing the risk of microvascular complications[27]. GHb was estimated by Ion-Exchange Chromatography Kit supplied by Crystal Chem, USA.

The homeostatic model assessment (HOMA) was used to assess changes in insulin resistance (HOMA-IR). This was calculated as follows HOMA-IR index = (FBG [in mmol/L] x FINS [in units/L]) /22.5[28].

Animals sacrifice

All rats were sacrificed at The Laboratory Animal House Unit of Kasr Al-Aini, Faculty of Medicine, Cairo University, by cervical dislocation after being anesthetized with IP injection of ketamine (90 mg/kg)/xylazine (15 mg/kg)[29]. The abdomens of all groups were opened and the pancreas was dissected. The tail regions of pancreas of all animals were divided into 3 slices one for pancreatic homogenates preparation, as previously described[30] for measurement of malondialdehyde (MDA), a lipid peroxidation indicator [expressed as mmol/mg tissue (MBS738685, MyBioSource, USA)]. The other two slices were for light and electron microscopic studies.

Histological Study

At Histology Department, Faculty of Medicine, Cairo University, the second pancreatic slice was fixed in Bouin solution and processed to Paraffin blocks. Paraffin sections 7 micrometers thick were cut. Unstained sections (from subgroups Ic, Id, group III &IV sacrificed 1 week after cellular injection) were examined by fluorescent microscope. The remaining sections from different subgroups scarified after two & six weeks were stained by:

1. Hematoxylin and Eosin stain (H&E)[31]
2. Immunohistochemical staining for:
    a. Caspase- 3: a rabbit polyclonal antibody, ab4051, abcam, USA: it appears as cytoplasmic reaction in the apoptotic cells.
    b. Insulin: a rabbit monoclonal antibody, ab181547, abcam, USA: it appears as brown cytoplasmic reaction in insulin producing cells.
    c. CD146: a rabbit monoclonal antibody, ab 75769, abcam, USA: it appears as membranous and cytoplasmic reactions in endothelial cells and pericytes[32,33].
    d. Sox9: a rabbit polyclonal antibody, ab26414, abcam, USA: transcription factor expressed in adult duct epithelium of pancreas and also considered as a marker and maintenance factor for pancreatic progenitors in ductal and centroacinar cells in adult rats. It appears as nuclear reaction[34,35].

Immunostaining using avidin–biotin technique required pretreatment[36] was carried out by 10 min boiling in 10 mM citrate buffer (cat no 005000) pH 6 for antigen retrieval. Then the sections were left to cool for 20 min in room temperature. Incubation of sections with the primary antibodies for one hour was performed. Immunostaining was completed using Ultravision One Detection System (cat no TL - 060- HLJ). Counterstaining was done using Lab Vision Mayer's hematoxylin (cat no TA- 060- MH). Citrate buffer, Ultravision One Detection System and Mayer's hematoxylin were purchased from Labvision, ThermoFisher scientific, USA. Based on data of antibody manufacturer, the positive tissues control for caspase-3 & insulin were specimen of liver pig and rat pancreas respectively and the reactions appeared cytoplasmic. For Sox9 the positive control was mouse spleen and the immunoreactivity was nuclear. For CD146 the positive tissue control was mouse spleen that exhibited membranous and cytoplasmic reactions. Negative controls were obtained by skipping step of adding the primary antibody.

The third slice was cut into small fragments (0.5- 1.0 mm3), prefixed in 2.5 % glutaraldehyde for 2 h. Then the fragments postfixed in 1% osmium tetroxide in 0.1 M phosphate buffer at pH 7.4 and 4 °C for 2 h. Dehydration and resin embedding were performed to obtain resin blocks[36]. Using a Leica ultracut (UCT) (Glienicker, Berlin, Germany) ultrathin (60–90 nm) sections were cut at Electron Microscope Research Unit, Faculty of Agriculture. Ultrathin sections were stained with uranyl acetate then lead citrate and examined by transmission electron microscope [TEM] (JEOL JEM-1400, Japan)[37]. For better visualization of pericytes by TEM, they were digitally colored green by Adobe Photoshop CC 2014.

Morphometric study

At Histology Department, Faculty of Medicine, Cairo University, image analysis by Leica Qwin-500 LTD-software image analysis computer system (Cambridge, England) was used to measure the area percent of caspase-3 and CD146 immuno positive reactions in islets measuring frame (105931.73µm2). The area percent of insulin and Sox9 immunoreactions was measured in the corresponding immunostained pancreatic sections. All measurements were done in ten non-overlapping fields (×100) for each animal of each subgroup. The count of PKH26 labelled AMSCs and ECFCs (×200) was analyzed in pancreatic sections using Image J Program.

Statistical analysis

All morphometric and biochemical measurements were expressed as mean ± standard deviation (SD) and were analyzed statistically using the software IBM Statistical Package for the Social Sciences (SPSS) version 21. This was performed using one-way analysis of variance (ANOVA) followed by "Tukey" Post Hoc test for all measurements except the count of PKH26 labelled AMSCs and ECFCs in which independent samples T-test was performed. The results were considered statistically significant when *P value* was < 0.05.

RESULTS

General observations

No deaths nor abnormal behavior was noticed in all rats except for the presence of excessive polyuria, as monitored by frequency to change cages, in the untreated diabetic subgroups and AMSCs-6Wsubgroup. The biochemical, histological and immunohistochemical results of all control subgroups were similar, so they were presented as group I.

Biochemical results (Figure 1)

All rats included in groups II, III &IV revealed blood glucose level above 16.7 mmol/L and were considered diabetic.

Fasting blood glucose (FBG), glycosylated hemoglobin (GHb), HOMA-IR and pancreatic MDA

The mean values of FBG, GHb, HOMA-IR and pancreatic MDA in T2D rats were significantly increased when compared to control rats. While their mean values after two weeks of injection with either AMSCs, or AMSCs+ECFCs showed significant decrease versus T2D rats and non significant difference versus the control group.

Regarding six weeks after AMSCs administration, these parameters expressed non significant decrease as compared to corresponded T2D rats and significant increase versus the control group. However, in combined group there was significant decrease in all measured parameters versus the corresponded T2D rats as well as AMSCs subgroup and non significant difference when compared to control group.

Fasting insulin (FINS)

Regarding the values of FINS, a significant decrease in all groups at the time of sacrifice (2&6 weeks) versus control group except AMSCs subgroup 2W and combined subgroups was recorded. There was significant increase in FINS 2 weeks after either AMSCs or AMSCs and ECFCs cotherapy versus the corresponded T2D subgroup. Meanwhile, at week 6, there was non significant increase in FINS in AMSCs treated subgroup and significant increase in combined subgroup versus T2D. Also, a significant increase in ECFCs combined subgroup versus AMSCs treated subgroup was observed.

Histological results

Fluorescent labelled sections

Pancreatic sections from subgroups Ic & Id showed absence of red fluorescent labelled cells (Figures 2a,b). Some labelled cells with PKH26 were detected in pancreatic sections of AMSCs treated group (Figure 2c), while in combined group many AMSCs and ECFCs cells were seen (Figure 2d).

Hematoxylin and Eosin stained sections

Control sections revealed normal structure of the pancreas. The exocrine part formed of secretory acini and ducts. The islets of Langerhans appeared as pale stained areas consisted of cords of polygonal cells with round vesicular nuclei separated by blood capillaries (Figure 3a).

Both T2D subgroups (2&6W) showed shrunken islets, many islet cells appeared swollen, and vacuolated, while others revealed deeply acidophilic cytoplasm. The nuclei were small darkly stained. Congested blood capillaries between islet cells were detected. Pancreatic ducts showed areas of epithelial stratification. Some acinar cells appeared vacuolated with small darkly stained condensed nuclei. Congested blood vessels were noted (Figures 3b,c).

As regards, AMSCs subgroup 2W and combined subgroups 2W&6W, pancreatic sections showed apparent normal islets cells apart from few cells with either vacuolated cytoplasm and or darkly stained nuclei. Sparse areas of epithelium stratification were observed in pancreatic ducts (Figures 3d,f,g).

Concerning AMSCs subgroup 6W, they revealed results comparable with T2D subgroups (Figure 3e)

Immunostained sections for caspase- 3

Examination of the pancreatic sections of control group revealed very few caspase-3 immunoexpression in islet cells and blood vessels (Figure 4a). Regarding T2D subgroups and AMSCs subgroup 6W, increased cytoplasmic immunoreactivity was noticed (Figures 4b,c,e). However in AMSCs subgroup 2W and combined subgroups, few caspase-3 positive cells were seen (Figures 4d,f,g).

Immunostained sections for insulin

Sections of control group showed positive cytoplasmic immunoreactivity in most of islets cells (Figure 5a). Sections of untreated diabetic subgroups (Figures 5b,c) and AMSCs subgroup 6W (Figure 5f) revealed very few immunoreactive cells. While sections of AMSCs-2W and combined subgroups 2&6W exhibited positive immunoreaction for insulin in most of the islets cells. Along with the presence of insulin positive cells close to pancreatic ducts (Figures 5d,e,g,h,i,j).

Immunostained sections for CD146

Sections of group I showed positive cytoplasmic and membranous immunoreactions in endothelial cells and pericytes of capillaries (Figure 6a). Regarding, T2D subgroups and AMSCs-6W recorded infrequent scattered immunoreactivity (Figures 6b,c,e). While apparent increased CD146 positive immunoreaction was demonstrated in AMSCs subgroup 2W and ECFCs cotherapy subgroups (Figures 6d,f,g).

Immunostained sections for Sox9

Control group revealed positive immunoreactivity in ductal and centroacinose cells for Sox9 antibody (Figure 7a). T2D subgroups as well as AMSCs-6W subgroup showed abundant Sox9 positive cells (Figures 7b,c,e). Several Sox9 immune expressions were observed in AMSCs-2W and in both combined subgroups (Figures 7d,f,g).

Ultra-thin sections (TEM)

Ultrastructurally, islet β-cells of control rats revealed euchromatic rounded nuclei, numerous secretory granules with characteristic electron dense core surrounded by electron lucent halo, numerous mitochondria, rough endoplasmic reticulum (rER) and Golgi apparatus (GA.). Cell junctions were also noted between adjacent cells.

Islet capillaries lined by ECs and surrounded by pericytes were seen in between islet cells. ECs had euchromatic nuclei, mitochondria and numerous vesicles in cytoplasm. Pericytes had cell body with discoid or kidney-shaped nuclei with peripheral heterochromatin and occasionally seen nucleoli, little cytoplasm usually contained small slender mitochondria, ribosomes and some rER. They had long foot processes emerged from cell bodies and some processes overlapped forming two or more layers embracing the ECs. Moreover, some pericytes were also seen in contact with several ECs. Pericytes had bands of filaments beneath the inner and outer plasma membranes, both near the nucleus and in the cytoplasmic processes. Regular continuous basement membranes that ensheath ECs and split to enclose pericytes were seen. The basement membrane between pericytes and ECs disappeared only at site of direct contact between pericyte and ECs (Figures 8 a,b).

The electron micrographs of pancreatic islets of both diabetic subgroups demonstrated lost granules in most of the cells leaving empty spaces or electron lucent areas. Few cells revealed granules with increased electron lucent halo around small electron dense cores. Nuclei of β-cells were variable, some were markedly shrunken and others had numerous clumps of heterochromatin with irregular nuclear envelope. GA and rER appeared dilated and the mitochondria were swollen, vacuolated with lost cristae (Figures 8 c-f).

Moreover, ECs in islet capillaries showed features suggestive of degeneration, they had nuclei with more condensed chromatin along the nuclear membrane, dense cytoplasm with swollen mitochondria and/or with ruptured cristae, numerous areas of vacuolations, few numbers of vesicles and occasional phagosomes. Capillary lumen appeared irregular and or narrowed with extensive protrusions (pseudopodia) of ECs into lumen. Furthermore, the ultrastructural alterations of islets pericytes varied from loss of pericytes contact with ECs and separation from ECs by thickened poorly organized basement membranes, detachment from basement membrane toward abluminal surface, and detection of either small fragments of foot processes or complete loss (Figures 8 d-f).

Sections of subgroups AMSCs -2W and AMSCs +ECFCs (2W&6W) demonstrated islet cells with preserved cell junctions, euchromatic nuclei with clumps of heterochromatin and many secretory granules of different sizes having electron dense core surrounded by lucent halo space. In addition, numerous rounded and elongated mitochondria as well as rER and GA with nearly normal appearance were noted throughout the cytoplasm. However, very few cells had shrunken irregular nucleus with peripheral heterochromatin, granules with increased halo spaces, mitochondria with ruptured cristae, dilated GA and rER (Figures 9a,b,d,e,f,g).

Furthermore, islet capillaries had apparently normal lumen and were lined by complete endothelial layer with typical tight junctions and several vesicles. Numerous elongated pericytes near or in direct contact with ECs and enveloped by apparently normal basement membranes were also observed. Added to that, some pericytes appeared with large cell bodies and large euchromatic nuclei with patches of heterochromatin. Their cytoplasm revealed mitochondria, rER, numerous ribosomes, either singly or in clusters and some vesicles (Figures 9 b,d,e,g).

The electron micrographs of subgroup AMSCs 6W supported the results seen by the light microscope, the attained improvement was greatly lost. Nuclei of islets cells appeared with numerous clumped heterochromatin and some irregularities in nuclear envelopes. Most of secretory granules were either empty or with increased halo spaces around small dense cores with few number of normal granules inbetween. Numerous destructed mitochondria as well as dilated GA and rER were detected. ECs of islet capillaries had areas of cytoplasmic vacuolations and some

pseudopodia. Pericytes and fragments of foot processes were seen within the basement memberanes (Figure 9 c).

Morphometric results

Mean number of PKH26 labelled cells was increased in combined group than AMSCs treated group and the difference was significant (Figure 2e).

Mean area % of caspase- 3 and Sox9 immunopositive cells was increased in all groups, but the difference was significant only in T2D & AMSCs-6W subgroups when compared to control. After 2weeks of cellular injection, there was significant decrease in AMSCs subgroup and combined subgroup versus T2D subgroup. However, after 6 weeks of cellular injection, there was only significant decrease in combined subgroup and non-significant decrease in AMSCs subgroup versus T2D subgroup. Moreover, a significant decrease in combined subgroup than that of AMSCs subgroup was noticed (Figures 4h,7h).

As regards the mean area % of immunopositive cells for insulin and CD146, significant decrease in all experimental subgroups except AMSCs 2W and combined subgroups 2 &6W versus the control group was detected. Moreover, significant increase in AMSCs 2W and combined subgroups than corresponded T2D subgroups was noticed. On the other hand, AMSCs subgroup 6W showed non-significant difference than respective T2D subgroup and significant decrease than that of combined subgroup 6W (Figures 5k,6h).

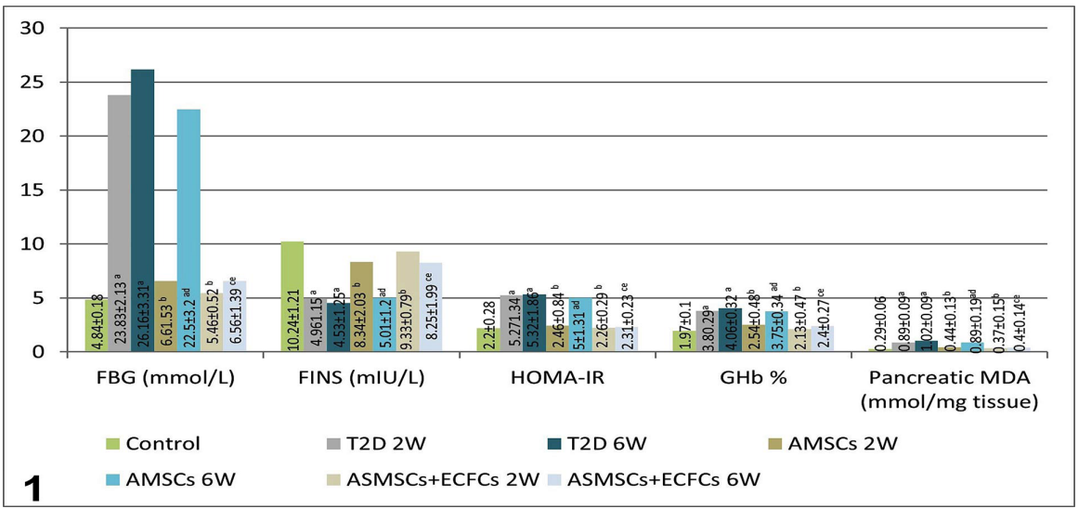

Fig. 1: Showing mean value of FBG, FINS, HOMA-IR, GHb % and MDA in all groups: a, b, c, d &e as compared to control group & subgroups T2D-2W, T2D-6W, AMSCs 2W &AMSCs 6W, respectively (significant difference at $P < 0.05$)

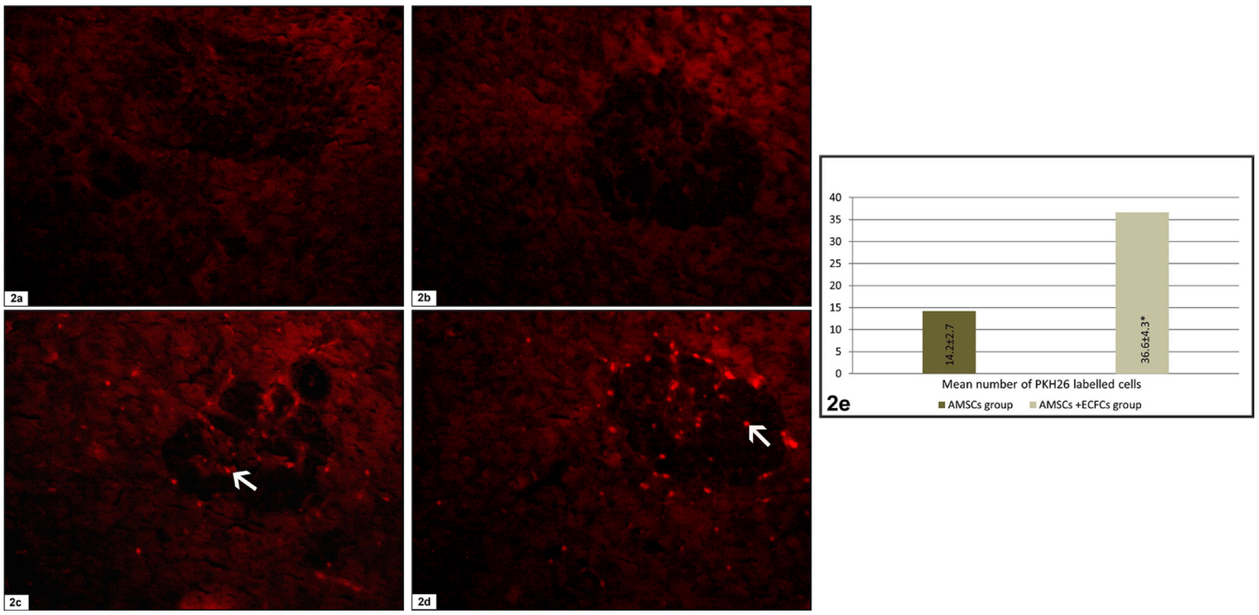

Fig. 2: Fluorescent microscope photomicrographs of pancreas sections showing: (a & b) Absence of red fluorescent of PKH26 labeled cells in pancreatic sections of subgroups Ic and Id. (PKH26 x 200). (c & d) Detection of some labelled cells (arrow) in group III and many labelled cells (arrow) in combined group. (PKH26 x 200). (e) Showing mean number of PKH26 labelled cells: * as compared to AMSCs group (significant difference at $P < 0.05$)

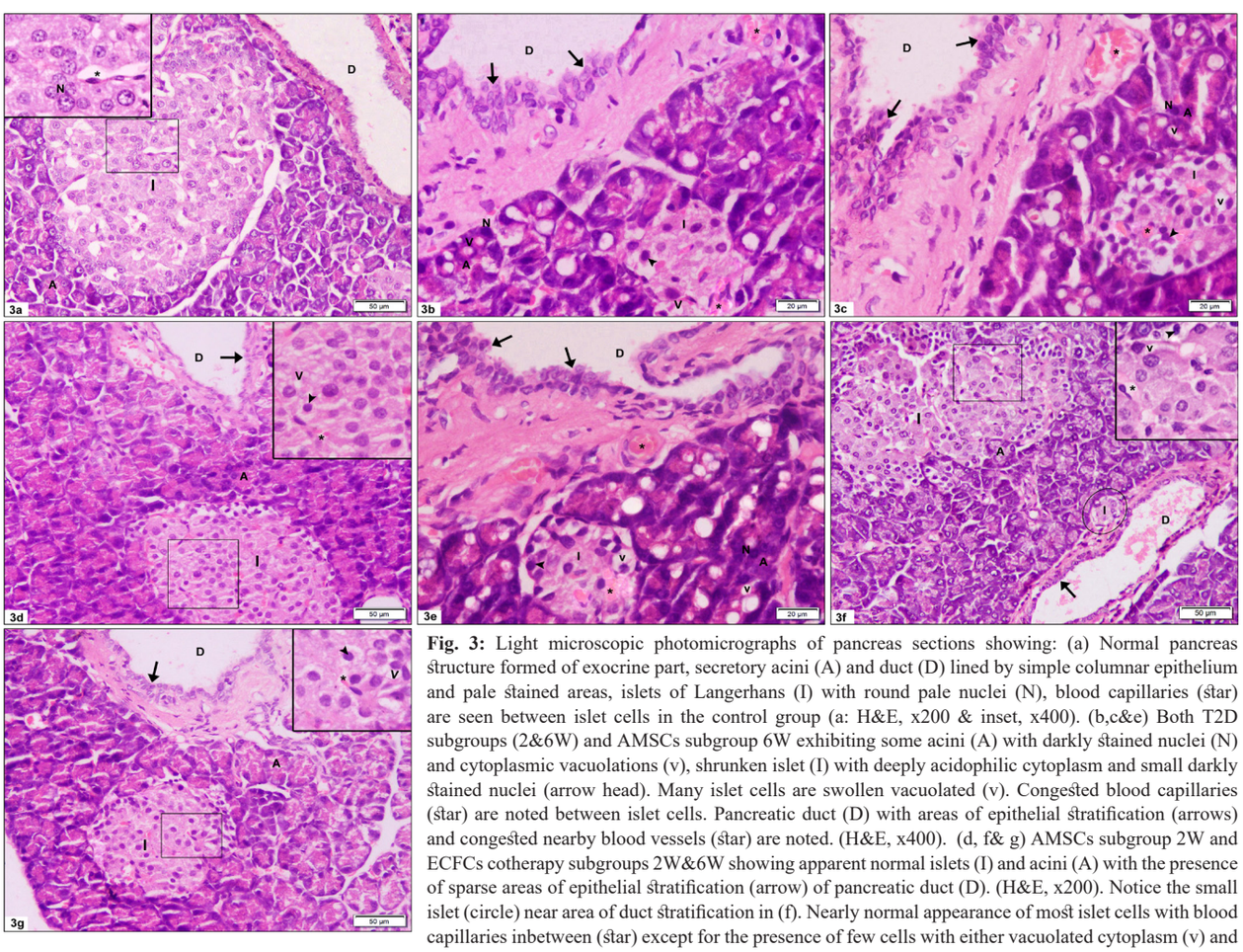

Fig. 3: Light microscopic photomicrographs of pancreas sections showing: (a) Normal pancreas structure formed of exocrine part, secretory acini (A) and duct (D) lined by simple columnar epithelium and pale stained areas, islets of Langerhans (I) with round pale nuclei (N), blood capillaries (star) are seen between islet cells in the control group (a: H&E, x200 & inset, x400). (b,c&e) Both T2D subgroups (2&6W) and AMSCs subgroup 6W exhibiting some acini (A) with darkly stained nuclei (N) and cytoplasmic vacuolations (v), shrunken islet (I) with deeply acidophilic cytoplasm and small darkly stained nuclei (arrow head). Many islet cells are swollen vacuolated (v). Congested blood capillaries (star) are noted between islet cells. Pancreatic duct (D) with areas of epithelial stratification (arrows) and congested nearby blood vessels (star) are noted. (H&E, x400). (d, f& g) AMSCs subgroup 2W and ECFCs cotherapy subgroups 2W&6W showing apparent normal islets (I) and acini (A) with the presence of sparse areas of epithelial stratification (arrow) of pancreatic duct (D). (H&E, x200). Notice the small islet (circle) near area of duct stratification in (f). Nearly normal appearance of most islet cells with blood capillaries inbetween (star) except for the presence of few cells with either vacuolated cytoplasm (v) and or darkly stained nuclei (arrow head). (H&E inset x400)

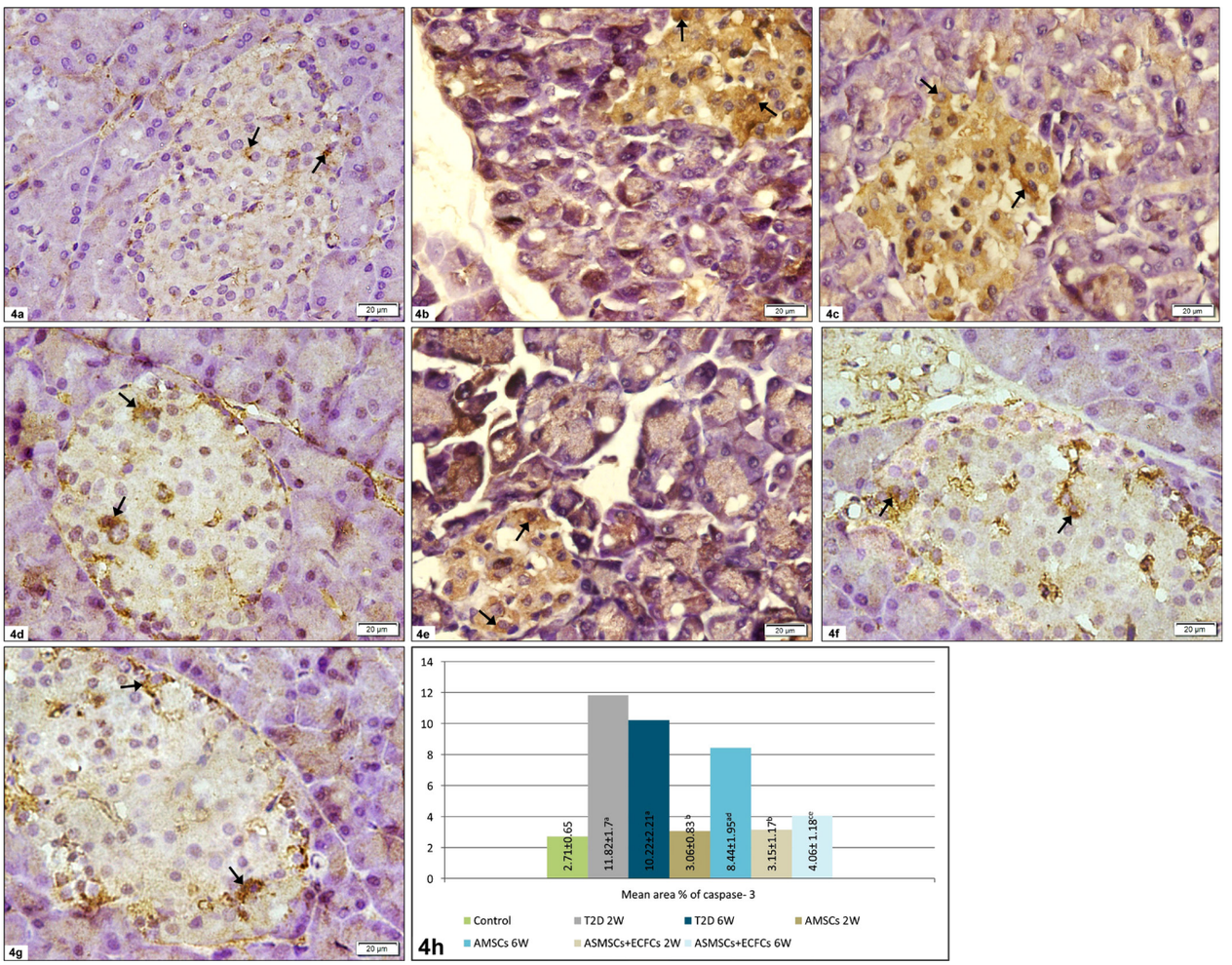

Fig. 4: Light microscopic photomicrographs of pancreas sections showing: (a) very few caspase-3 immunoreaction (arrows) in control islet. (b,c&e) T2D subgroups (2&6W) and AMSCs subgroup 6W showing multiple cytoplasmic immunoreactivity (arrows). (d,f&g) AMSCs subgroup 2W and ECFCs cotherapy subgroups 2W&6W illustrating few caspase-3 positive cells (arrows). (Anti caspase 3 immunohistochemical stain, x400). (h) Showing mean area % of caspase 3 immuno positive cells: a, b, c, d &e as compared to control group & subgroups T2D-2W, T2D-6W, AMSCs 2W &AMSCs 6W, respectively (significant difference at $P < 0.05$)

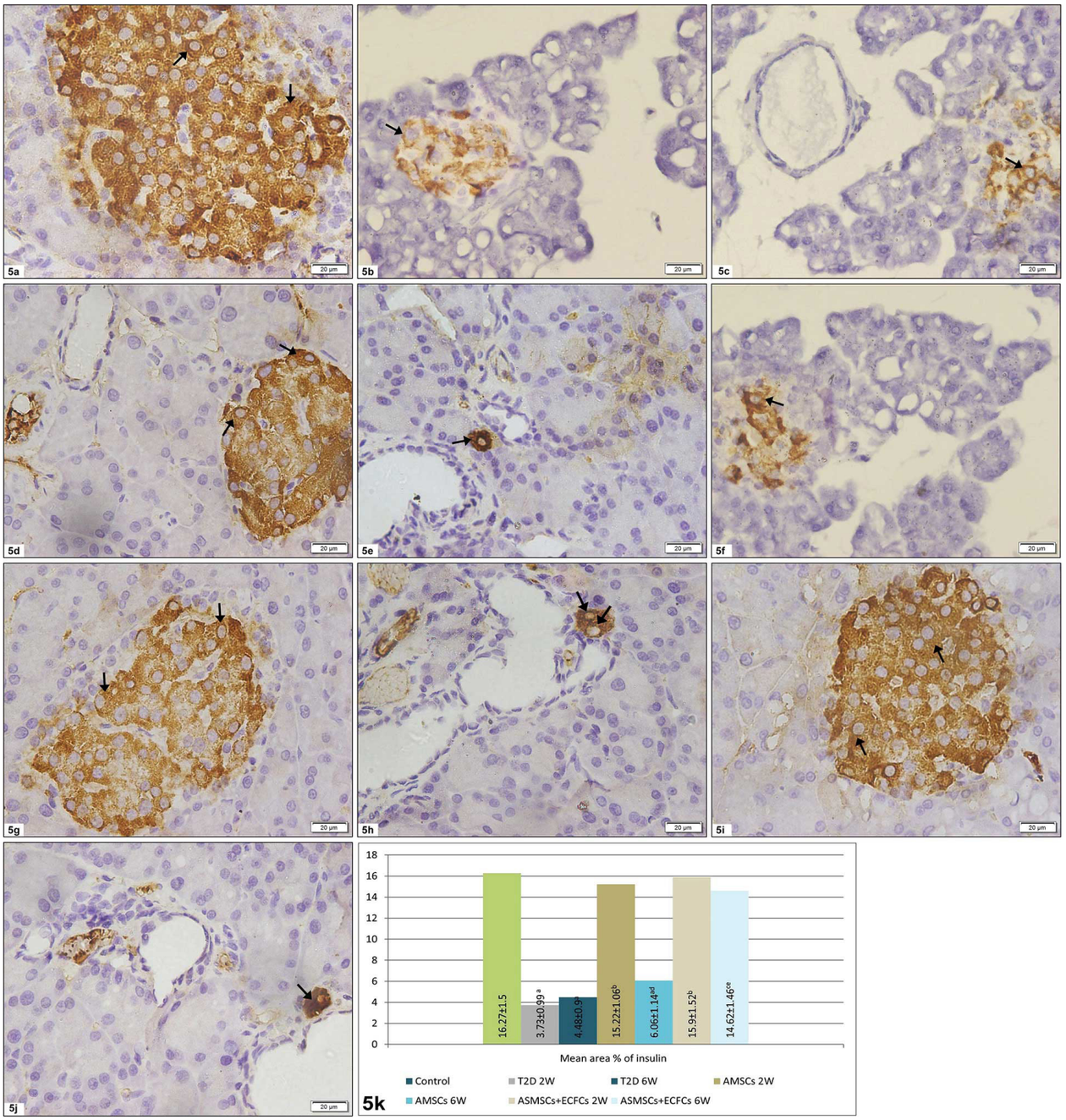

Fig. 5: Light microscopic photomicrographs of pancreas sections showing positive insulin cytoplasmic immunoreaction (arrows) in: (a, d, g&i) Most of islets cells in control group and AMSCs-2W and ECFCs-2&6W subgroups. (b,c&f) very few immunoreactive cells in T2D subgroups (2&6W) and AMSCs subgroup 6W. (Anti insulin immunohistochemical stain, x400). (e,h&j) Insulin positive cells near pancreatic ducts are noted in AMSCs-2W and ECFCs-2&6W subgroups respectively. (Anti insulin immunohistochemical stain, x400). (k) Showing mean area % of insulin immuno positive reaction: a, b, c, d &e as compared to control group & subgroups T2D-2W, T2D-6W, AMSCs 2W &AMSCs 6W, respectively (significant difference at $P < 0.05$)

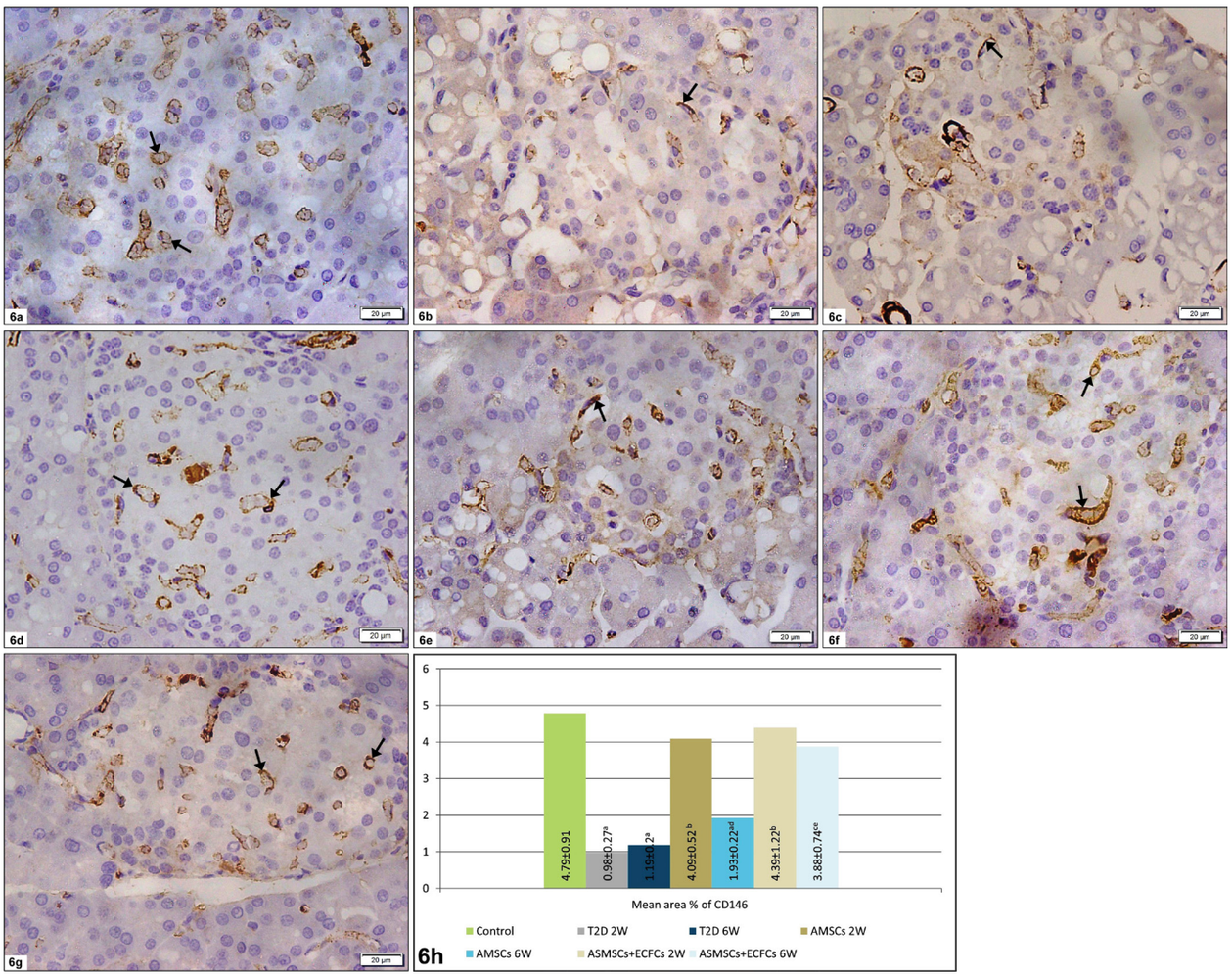

Fig. 6: Light microscopic photomicrographs of pancreas sections showing positive CD146 cytoplasmic and membranous immunoreactions (arrows) in endothelial cells and pericyte of islets capillaries in: (a) Control group. (b,c&e) infrequent scattered immunoreaction in T2D subgroups (2&6W) and AMSCs subgroup 6W. (d,f&g) Apparent increased CD146 positive immunoreactivity in AMSCs subgroup 2W and ECFCs cotherapy subgroups 2&6W. (Anti CD146 immunohistochemical stain, x400). (h) Showing mean area % of CD146 immunoreactivity: a, b, c, d &e as compared to control group & subgroups T2D-2W, T2D-6W, AMSCs 2W &AMSCs 6W, respectively (significant difference at $P < 0.05$)

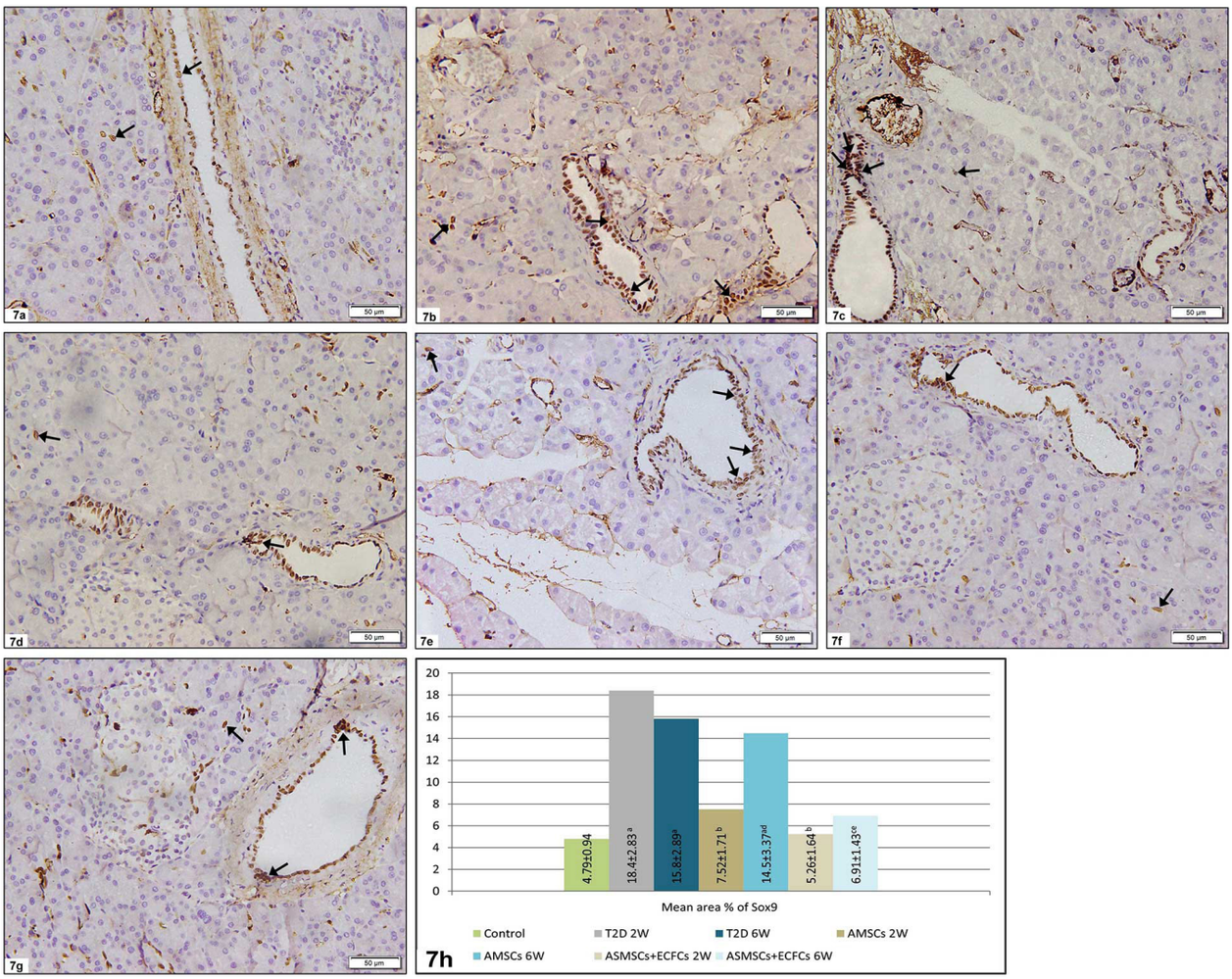

Fig. 7: Light microscopic photomicrographs of pancreas sections showing positive SOX9 cytoplasmic immunoreactions (arrows) in ductal and centroacinose cells: (a) Control group. (b,c&e) abundant immunopositive cells in T2D subgroups and AMSCs-6W subgroup. (d, f&g) Several immune expressions in AMSCs-2W and in ECFCs-co-transplanted subgroups 2&6W. (Anti SOX9 immunohistochemical stain, x200). (h) Showing mean area % of SOX9 immunoreactivity: a, b, c, d &e as compared to control group & subgroups T2D-2W, T2D-6W, AMSCs 2W &AMSCs 6W, respectively (significant difference at $P < 0.05$)

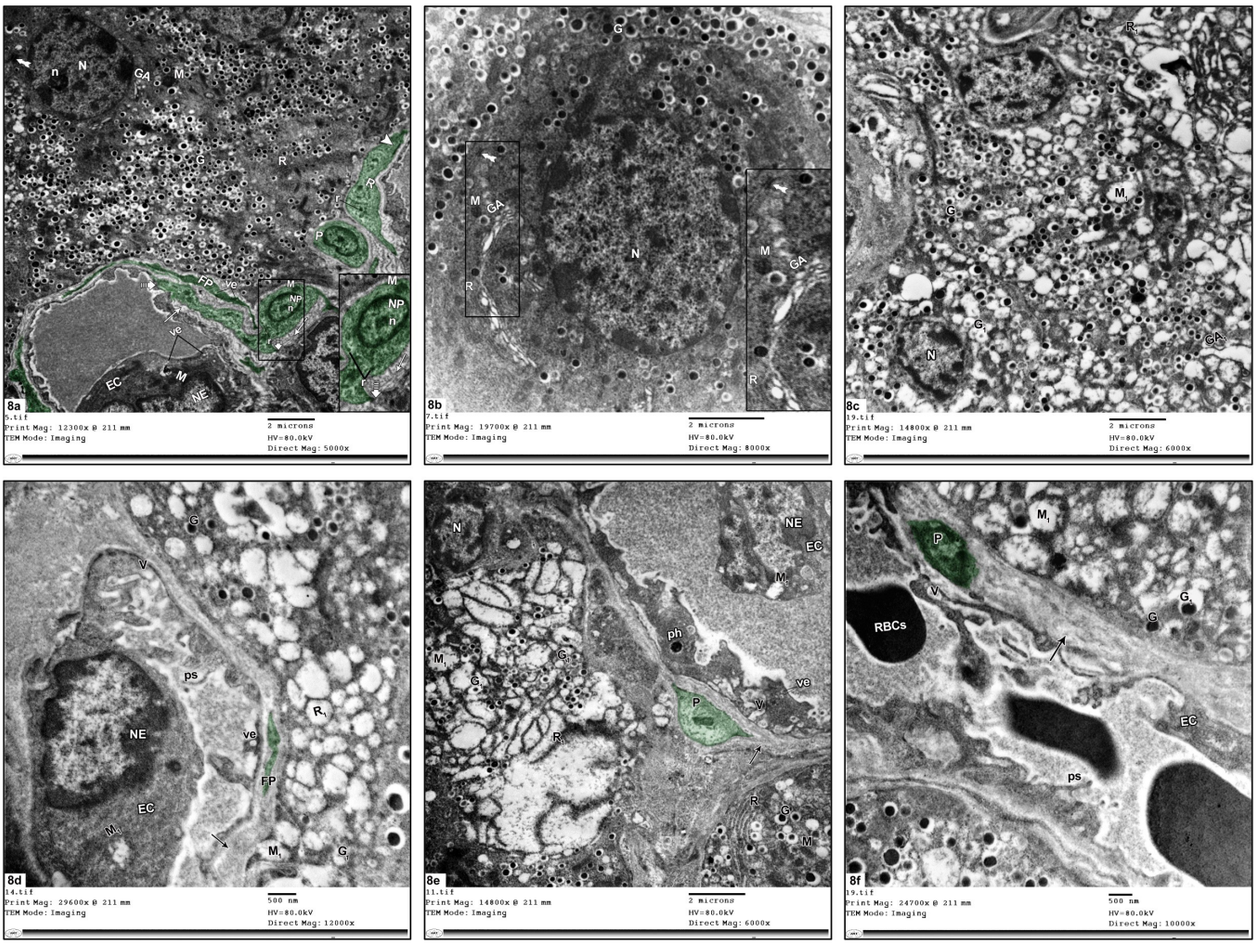

Fig. 8: TEM photomicrographs of pancreatic islets in control group& T2D (subgroups -2W& -6W): (a&b): Control group: β-cells having euchromatic rounded nuclei (N) with prominent nucleoli (n) and multiple secretory granules (G) with characteristic electron dense core surrounded by wide electron lucent halo. Mitochondria (M), rough endoplasmic reticulum (R) and Golgi apparatus (GA) with normal ultrastructure are present among the secretory granules. Cell junctions (bifid arrow) are also noted between adjacent β- cells. Islet capillaries lined by endothelial cells (EC) with euchromatic nucleus (NE), mitochondria (M) and numerous vesicles (ve) are seen. Pericytes (P) (digitally colored in green) having discoid nuclei (NP) with peripheral heterochromatin and nucleoli (n), mitochondria (M), rER (R), ribosomes (r) and long foot processes (FP) with bands of filaments (arrow head), some processes are overlapping forming two or more layers, are observed in contact with ECs. Regular continuous basement membranes (arrow) ensheath ECs and split to enclose pericytes. Notice sites of direct contact (dashed arrow) between pericytes and ECs (TEM a:x5000, inset x12000 & b:x8000, inset x15000).
(c) T2D subgroup 2W revealing β-cells with shrunken nuclei (N) with patches of heterochromatin, dilated rER (R1) and GA (GA1) and destructed mitochondria (M1). Most of granules (G1) are either empty or with increased halo spaces around small dense cores. Some granules (G) are apparently normal (TEMx6000).
(d) Another field of T2D subgroup 2W showing irregular narrow capillary lumen revealing swollen endothelial cell (EC) with extensive pseudopodia (ps), nucleus (NE) with peripheral heterochromatin, dense compact cytoplasm contained partially swollen mitochondria (M1) with destructed cristae, vacuolations (V) and few vesicles (ve). Only small fragment of pericyte foot process (FP) (digitally colored in green) is seen within thickened and poorly organized basement membrane (arrow). β- cell has mitochondria (M1) with lost cristae, dilated rER (R1) and empty granules (G1) or with electron dense cores surrounded by large electron lucent halo. Few normal granules (G) are also noted (TEMx12000).
(e) T2D subgroup 6W illustrating β-cell with markedly shrunken nucleus (N) with clumps of heterochromatin, extensive dilated rER (R1), swollen mitochondria (M1) with destructed or lost cristae, most of granules (G1) are empty or having small electron dense cores surrounded by large electron lucent halo. Another part of beta cell with some normal granules (G), mitochondria (M) and rER (R) are also noted. Endothelial cell (EC) bulging in blood capillary lumen shows nucleus (NE) with clumps of heterochromatin, dense cytoplasm with some vesicles (ve), phagosome (ph), numerous vacuolations (V) and swollen mitochondria (M1) with ruptured cristae. Pericyte (P) (digitally colored green), with loss of foot process, is separated from EC by thickened basement membrane (arrow) (TEMx6000). (f) T2D subgroup 6W illustrating islet capillary shows endothelium (EC) with extensive pseudopodia (ps) and numerous large vacuolations (V). Pericyte (P) (digitally colored in green), with loss of foot process, is noted enclosed by thickened basement membrane (arrow). RBCs are seen within the capillary lumen. Two parts of β-cells reveal numerous swollen mitochondria (M1) with destructed or lost cristae and granules (G1) with increased electron lucent halo. Note few normal granules (G) (TEMx10000)

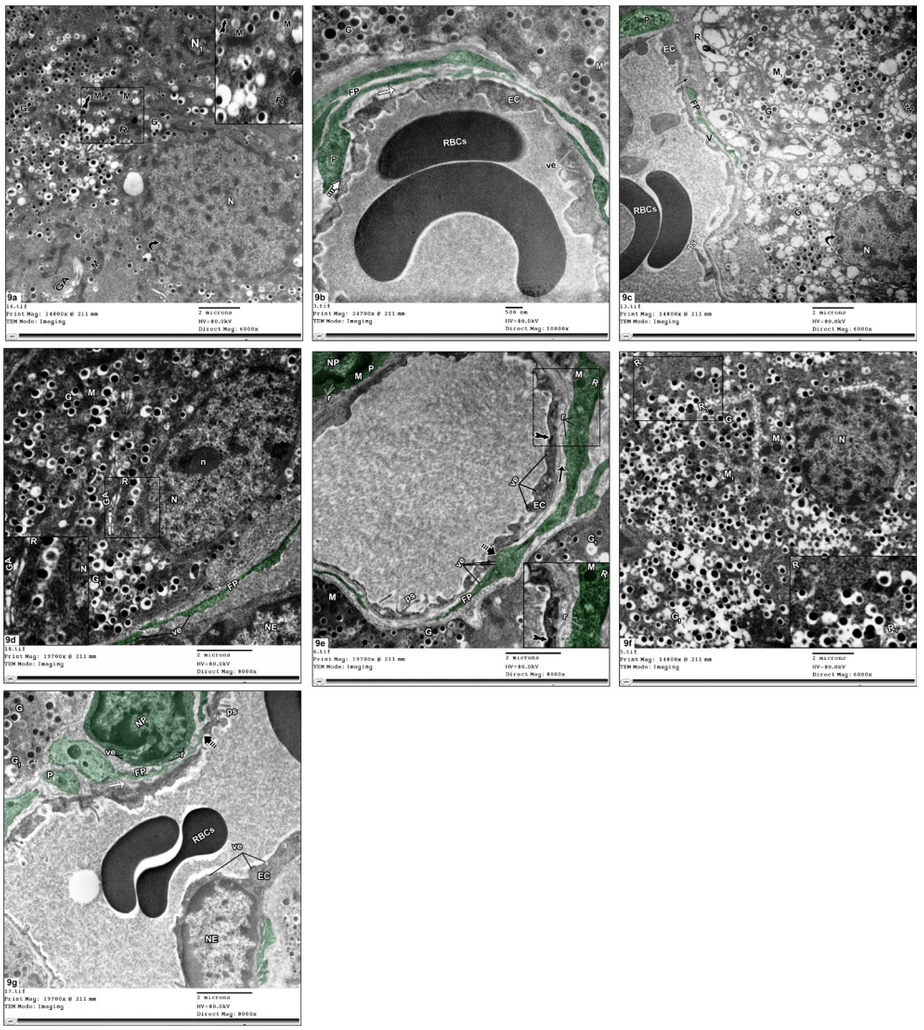

Fig. 9: TEM photomicrographs of pancreatic islets in AMSCs (2W&6W subgroups) & ECFCs (2W&6W subgroups): AMSCs-2W illustrating: (a): β-cells with preserved cell junctions (bifid arrow), euchromatic rounded nucleus (N) having clumps of heterochromatin and some irregularities in nuclear membrane (curved arrow) and apparently normal secretory granules (G), mitochondria (M), rER (R) and GA (GA). A shrunken irregular nucleus (N1) with peripheral heterochromatin, some granules (G1) with increased halo spaces around small dense cores or empty and mitochondria (M1) with ruptured cristae are also noted (TEMx6000& inset x12000). (b): Islet capillary with restored lumen and complete endothelial layer (EC), some vesicles (ve), several pericytes (P) and their foot processes (FP) (digitally colored in green) in direct contact (dashed arrow) with EC are noticed within the basement membrane (arrow). RBCs are also seen. A part of β-cell with normally appeared secretory granules (G) and mitochondria (M) is observed (TEMx10000). (c) AMSCs-6W illustrating islets cell with nucleus (N) having numerous clumped heterochromatin and irregular nuclear envelope (curved arrow), dilated GA (GA1), dilated rER (R1) and swollen, vacuolated mitochondria (M1) with lost cristae. Granules (G1) are lost leaving empty spaces or having small electron dense cores surrounded by large electron lucent halo. A small number of apparently normal granules (G) are also seen. Endothelial cell (EC) lining blood capillary shows vacuolations (V) and some pseudopodia (ps). A pericyte (P) and small part of pericyte foot process (FP) (digitally colored in green) are seen within the basement membrane (arrow). Note the shreds of ECs and RBCs in capillary lumen (TEMx6000). (d): ECFCs-2W demonstrating β-cells with euchromatic oval nucleus (N) having prominent nucleolus (n). Most of granules (G), mitochondria (M), rER (R) and GA (GA) appear normal. Few empty secretory granules (G1) are noted. Also, a foot process (FP) of pericyte (digitally colored in green), with vesicles (ve), in the basement membrane (arrow) and part of endothelial nucleus (NE) are noticed (TEMx8000 &inset x15000). (e): Islet capillary in ECFCs-2W, with apparently normal lumen and complete endothelial layer (EC) having preserved tight junctions (bifid arrow), multiple vesicles (ve), some pseudopodia (ps) and surrounded by basement membrane (arrow) enclosing a long foot processes of pericyte (FP) (digitally colored in green) containing numerous ribosomes (r), rER (R), mitochondria (M) and many vesicles (ve) and in direct contact (dashed arrow) with EC. Also, a pericyte (P) containing euchromatic nucleus (NP) with peripheral heterochromatin, mitochondria (M) and numerous ribosomes (r) is seen. Moreover, a part of β-cell; with normally appeared mitochondria (M) and secretory granules(G) apart from few empty granules (G1); is also observed (TEMx8000 & inset x15000). (f) ECFCs-6W revealing: β-cell with euchromatic oval nucleus (N) with clumps of heterochromatin, many secretory granules of variable sizes showing electron dense core surrounded by lucent halo (G) and apparently normal mitochondria (M) and rER (R). Also, some granules (G1) have widened halo or completely empty, mitochondria (M1) have destructed cristae and some slightly dilated rER (R1) are observed (TEMx6000& inset x12000). (g): Islet capillary in ECFCs-6W, with apparently restored lumen containing RBCs, lined by endothelial cell (EC) with euchromatic nucleus (NE), numerous vesicles (ve) and some pseudopodia (ps), is seen. Many pericytes (P) and their foot processes (FP) (digitally colored in green) close to or in direct contact (dashed arrow) with EC are noticed within the basement membrane (arrow). One pericyte has large slightly indented euchromatic nucleus (NP) with peripheral heterochromatin and, numerous ribosomes (r) and vesicles (ve). Parts of β-cells; with normally appeared secretory granules (G) and few empty granules (G1) (TEMx8000)

DISCUSSION

Type 2 diabetes is a chronic metabolic disease[38] associated with hyperglycemia, insulin resistance, and dyslipidemia[39]. Hyperglycemia in diabetic patients predispose to endothelial dysfunction[40] and impaired angiogenesis[41].

In this study, high fat diet combined with STZ administration induced T2D with progressive β cell dysfunction[15]. Male rats were chosen for induction of T2D model as they were more sensitive to diabetogenic action of STZ[42]. STZ administration destroys islet cells through several mechanisms, including production of reactive oxygen species, induction of immune and inflammatory responses[43], accelerated metabolic stress (glucosamine pathway activity, stimulated glucolipotoxicity & elevated glycation) and increased endoplasmic reticulum stress that results in β cell death by apoptosis[44,45].

Islet cells apoptosis in T2D rats of the current study was illustrated histologically by apoptotic features; deeply acidophilic cytoplasm and small darkly stained nuclei and was confirmed immunohistochemically by the significant increase in mean area % of caspase- 3 positive islet cells as compared to the control group. This was in line with previous study[15].

Other islet cells were swollen with cytoplasmic vacuolations, granules appeared with either small electron dense cores and increased electron lucent halo or empty, dilated GA and rER and swollen mitochondria with lost cristae indicating necrosis that might be attributed to lipid peroxidation[46]. That was proved by significant increase in pancreatic MDA versus control group.

The above mentioned degenerative changes of islets cells were reflected biochemically as significant decrease in FINS and significant elevation in FBG, GHb and HOMA-IR in T2D subgroups versus the control group. This was confirmed immunohistochemically by significant decrease in the mean area percent of insulin producing cells as compared to the control group and was in accordance with a former study[15].

Added to that, in the adult pancreas, islets rely on their dense capillary network to respond adequately to changes in blood glucose levels[47]. However, a decrease in islet vascular density was documented in different T2D animal models[48] with loss of islets control on own blood supply resulting in inadequate insulin release into the circulation and thus worsening the glycemic control[49]. Consistent with these findings, T2D subgroups in the present work recorded significant decrease in mean area percent of CD146 immuno-positive reactive islets vasculature cells versus the control group.

Endothelial cells impairment in the present work was furtherly emphasized by caspase- 3 immuno-positive cells of islet capillaries and by their ultrastructural changes where they appeared with dense cytoplasm, numerous pseudopodia and areas of vacuolations, ruptured cristae of mitochondria and few vesicles with thickened capillaries basement membranes. These findings were reported also in a previous study which added thickening and fragmentation of islet capillaries and endothelial cells[7]. Such endothelial alteration was considered as an early event in the pathogenesis of hyperglycaemia[48] and as an influential contributor to the impairment of secretory function and survival of β cell in type 2 diabetes[7].

Furthermore, capillary congestion and dilatation recorded in our study could be considered as an attempt to adapt to insulin resistance and exaggerated insulin demand in T2D by increasing insulin delivery into the peripheral circulation[50,51]. This observation was formerly noticed where they linked it to the pancreatic microcirculatory; endothelial cells and pericytes; disturbances and oxidative stress production[51,52].

The observed thickened capillaries basement membranes in T2D subgroups was demonstrated formerly[51] where they associated islet capillary dilation with basement membrane remodeling leading to inability to maintain capillary function and consequently β-cell damage. Moreover, other fields in the current work showed irregular and narrowed islet capillaries that could be explained by swollen endothelial cells with extensive pseudopodia. This was illustrated in a previous study[48]

Knowing that, endothelial cells and pericytes share the same basement membrane[49,53] and interact through the closely opposed foot processes and adherent junctions[48]. The present work assumed loss of cross link between these cells in T2D subgroups as indicated by loss of pericyte foot processes and contact with endothelial cells. This assumption goes along with an earlier study and was attributed to the current state of hyperglycemia and oxidative stress[49].

Examination of different histological sections of T2D rats showed areas of epithelial stratification in pancreatic ducts. Following pancreatic injury, activation of progenitors located in the ductal lining epithelium is a trial to replace the lost β cells[54]. This idea was supported in the present study by significant increase in mean area percent of Sox9 positive cells in these subgroups versus control, but this was not accompanied by parallel increase in mean area percent of insulin producing cells indicating failure of trans-differentiation, probably due to improper microenvironment.

After 2weeks of either AMSCs or AMSCs+ ECFCs cotherapy in the present study, amelioration of β cells was recorded. This amelioration could be verified by the nearly normal histological structure of the islets of Langerhans, preserved ultrastructure of β cells, abundant positive insulin immunoreactions and the significant increase in its mean area percent and serum level of FINS compared to T2D. The current study attributed this improvement to AMSCs as non significant difference was observed in different parameters between AMSCs and combined subgroups. This assumption was strengthened previously as AMSCs

infusion improved hyperglycemia by recovering islet cells[22,55].

Such improvement was formerly suggested to occur through different mechanisms. The first could be through differentiation of AMSCs into insulin-producing cells (IPCs) as numerous transcription factors like insulin gene enhancer protein (Isl-1) and Pax-6 were expressed in AMSCs[56]. This could be supported in the present work by homing of PKH26 labelled AMSCs into the pancreas, one week after their intravenous injection in both subgroups, and by the preserved function of pancreatic β cells 2 weeks after injection. Similarly, in a prior study, homing of GFP labelled AMSCs in pancreas tissues was observed 1 and 2 weeks after injection followed by differentiation into β cells. However, the number of homed cells was believed to be insufficient solely to explain this improvement[57]. Therefore, another postulated mechanism by which AMSCs improved T2D was the release of several cytokines, anti-inflammatory and antiapoptotic molecules that reduced pancreatic β-cell death[22]. This cytoprotecive effect was proved in the current study by significant decrease in pancreatic MDA level and mean area % of caspase- 3 immunopositive islet cells in both treated subgroups versus T2D-2Wsubgroup.

Furthermore, the significant decrease in mean values of FBG, GHb and HOMA-IR in these treated rats compared to T2D subgroup can be referred to insulin-sensitizing effects of AMSCs as they could restore expression of insulin receptors and peroxisome proliferator-activated receptors in livers and suppress pro-inflammatory cytokine expression as IL-6& TNF-α in insulin-targeting tissues which in turn, improve glucose and insulin sensitivity[57].

Similarly, the previously mentioned cytoprotecive effect and the capability of AMSCs to differentiate into endothelial cells[58] and pericytes[59] could explain the noticed restoration of islets' microvasculature in these treated subgroups. This was evidenced by the demonstrated apparently normal appearance of endothelial cells and pericytes by electron microscopy, few caspase-3 positive cells and by the significant increase in CD146 immunoreactions in islets' vasculature compared to corresponded T2D.

A remarkable observation in the present work was the appearance of insulin positive cells nearby duct epithelium in AMSCs-2W and combined 2W subgroups. Possibilities of this might be through differentiation of AMSCs or induction of recruitment and differentiation of endogenous pancreatic stem cells. Stimulation of duct stem cells proliferation in the present work might be assumed by presence of few stratification areas of pancreatic duct epithelium that was supported by increased Sox9 expression compared to control with subsequent differentiation into functional β cells. This was enforced by appearance of insulin positive cells near to the duct epithelium with diminished Sox9 expression compared to corresponded T2D. This could be attributed to the fact that expression of Sox9, a crucial transcription factor for maintenance of pancreatic progenitors[60], is dynamic and diminishes with trans-differentiation[61]. This was in consistent with Rezanejad and colleagues who proposed that duct epithelial cells can differentiate into functional β cells[35].

Unfortunately, the histological improvement and the accompanied hypoglycemic effect caused by single AMSCs infusion lasted for 2 weeks; after wards, AMSCs-6w subgroup revealed non significant difference in mean area percent of insulin and caspase- 3 immunopositive islet cells versus T2D-6W. In addition, the pancreatic MDA and blood glucose level, GHb and HOMA-IR regained a higher level concomitant with the decrease in serum insulin concentration. This limited and short term improvement was similarly reported in various studies[8,13] where they referred it to the short half- life of MSCs, the nature of T2D as a chronic progressive disease[13] and to the state of hyperglycemia and metabolic disturbance in diabetic microenvironment around AMSCs which impede their effectiveness[62].

Therefore, developing new strategies to enhance and prolong stem cells efficiency in regulating metabolic disorders in T2D is essential. For this reason, the second hypothesis addressed by present work was whether cotherapy with ECFCs can improve this microenvironment and furtherly potentiate and prolong the effect of AMSCs or not. This type of cells was chosen as they are highly proliferative cells in *vitro*, and their combination has been shown to form enduring, well perfused microvascular networks that improved ischemia in models of hind limb ischemia and myocardial infarction[63].

Compared with AMSCs 6w subgroup, rats cotherapy with ECFCs attained significantly decreased values of pancreatic MDA, FBG, GHb and HOMA-IR, caspase- 3 positive islet cells, that paralleling the significant increase in mean area percent of insulin producing cells. Finally increase in peripheral insulin sensitivity. Collectively, these results demonstrated that homed ECFCs at pancreas, by detection of more PKH26 labeled cells in this group, prolonged and enhanced the effects of AMSCs in improving glucose homeostasis in T2D. These augmented effects were previously noticed and attributed to the ability of ECFCs to preserve the stemness properties of MSC and reduce their early apoptosis[64] and modulate their regenerative potentials by paracrine secretion of angiocrine factors[65] creating a vascular niche in which the crosstalk between endothelial cells and β cells is necessary for proper pancreatic differentiation and β cell development and function[66]. Also, through ECFCs production of multiple paracrine factors as transforming growth factor beta (TGFβ)[67] and hepatocyte growth factor (HGF)[68] that modulate gene expression, proliferation, and survival of β cells.

This prolonged regenerative effect of ECFCs-6w on islet vascularity was demonstrated in the present work

ultrastructurally by restored nearly normal appearance of endothelial cells and pericytes and immunohistochemically by decreased caspase- 3 positive cells and preserved CD146 mean area percent. This could be attributed to the ability of ECFCs to maintain the capillary integrity by incorporation into the disrupted endothelium and differentiation into endothelial cells[69] and via promoting MSC differentiation not only to endothelial cells but also into pericytes[70]. Interaction of pericytes with endothelial cells during tissue repair play a crucial role for proper vascular function, by providing structural stability, participating in angiogenesis, and controlling vascular permeability and blood flow[53,71]. This fact was shown histologically in control group where single pericyte appeared in contact with several ECs, also extending their cytoplasmic processes to more than one vessel enforcing that pericytes may integrate and mediate some ECs functions. Such interaction was more highlighted in subgroups treated by ECFCs by observing numerous pericytes communicating with endothelium, attaining some of them angiogenic characters as enlarged cell bodies, euchromatic nuclei, rER, numerous ribosomes and vesicles[72]. Further enforcement came from the recorded significant and maintained increase in mean area % of immunopositive cells for CD146. CD146 not only endothelial biomarker for angiogenesis, but it also coordinates endothelial cell-pericyte communication for proper vessel integrity[32] as it is expressed by pericytes to function as a co-receptor for binding of PDGF-β secreted by endothelial cells. This binding induces pericytes recruitment and adhesion to endothelium and vessel stabilization[33,53,73]. In the same context, the restored pericytes were supposed to participate in the observed improvement of pancreatic islets' function as it was reported that pericytes able to directly control the maintenance of β cell maturity and glucose homeostasis by expression of certain factors to promote β cell function[6] and by release of nerve growth factor which stimulate exocytosis of insulin granules[74].

Mutually, AMSCs support and stabilize these ECFCs-derived neovessels by release of proangiogenic factors to aid long-term neovascularization and regenerative process[75].

Added to the previously reported regenerative effects of ECFCs, multiple researches demonstrated that ECFCs favor differentiation of ductal progenitor cells to somatic cell types via a paracrine manner through release of trophic factors as TGF-β, PDGF-B, VEGF and angiopoietins[76,77] and by exosomes which transfer information (mRNA, miRNA, DNA) between the cells[78]. This might enforce the observed significant decrease in Sox9 area percent in this subgroup compared to AMSC 6W and declare the target of ECFCs therapy especially for prolonged reparative effect, as it was documented that differentiation of Sox9 positive ductal cells into β-cell is a slow process and needs long-term growth factor therapy[79].

Taken together from all the aforementioned studies, tissue-regeneration on attributes of ECFCs are not strictly dependent on neovascularization ability but also on the trophic capacity to create a microenvironment that encourage a regenerative phenotypical switch in tissue-resident somatic cells[16].

CONCLUSION

ECFCs cotherapy with AMSCs enhanced and prolonged the anti-diabetic effects of AMSCs in T2D rats, and this effect was mediated by the enhancement of islets regeneration, islets' vasculature and probably by duct epithelium trans-differentiation.

CONFLICT OF INTERESTS

There are no conflicts of interest.

REFERENCES

1. Khan MAB, Hashim MJ, King JK, Govender RD, Mustafa H, Al Kaabi J. Epidemiology of Type 2 Diabetes - Global Burden of Disease and Forecasted Trends. J Epidemiol Glob Health. 2020; 10:107-11.

2. Gheibi S, Samsonov AP, Gheibi S, Vazquez AB, Kashfi K. Regulation of carbohydrate metabolism by nitric oxide and hydrogen sulfide: Implications in diabetes. Biochem Pharmacol. 2020; 176:113819.

3. Kalsi DS, Chopra J, Sood A. Association of lipid profile test values, type-2 diabetes mellitus, and periodontitis. Indian J Dent. 2015; 6: 81-4.

4. Xi Y and Bu: Stem Cells Therapy in Diabetes Mellitus. J Stem Cell Res Ther. 2014; 4:199.

5. Peiris H, Bonder CS, Coates PT, Keating DJ, Jessup CF. The β-cell/EC axis: how do islet cells talk to each other?. Diabetes. 2014; 63:3-11.

6. Sakhneny L, Rachi E, Epshtein A, Guez HC, Wald-Altman S, Lisnyansky M, Khalifa-Malka L, Hazan A, Baer D, Priel A, Weil M, Landsman L. Pancreatic pericytes support beta-cell function in a Tcf7l2-dependent manner. Diabetes. 2018; 67:437–47.

7. Hogan MF and Hull RL. The islet endothelial cell: a novel contributor to beta cell secretory dysfunction in diabetes. Diabetologia. 2017; 60:952-9.

8. Gao J, Cheng Y, Hao H, Yin Y, Xue J, Zhang Q, Li L, Liu J, Xie Z, Yu S, Li B, Han W, Mu Y. Decitabine assists umbilical cord-derived mesenchymal stem cells in improving glucose homeostasis by modulating macrophage polarization in type 2 diabetic mice. Stem Cell Res Ther. 2019; 10:259.

9. Kandaswamy R, Skeans MA, Gustafson SK, Carrico RJ, Tyler KH, Israni AK, Snyder JJ, Kasiske BL. OPTN/SRTR 2013 Annual Data Report: pancreas. Am J Transplant. 2015; 15:1-20.

10. Zang L, Hao H, Liu J, Li Y, Han W, Mu Y. Mesenchymal stem cell therapy in type 2 diabetes mellitus. Diabetol Metab Syndr. 2017 15; 9:36.

11. Mangin G, Poittevin M, Charriaut-Marlangue C, Giannesini C, Merkoulova-Rainon T, Kubis N. Glatiramer acetate reduces infarct volume in diabetic mice with cerebral ischemia and prevents long-term memory loss. Brain Behav Immun. 2019; 80:315-27.
12. Sempere JM, Martinez-Peinado P, Arribas MI, Reig JA, De La Sen ML, Zubcoff JJ, Fraga MF, Fernández AF, Santana A, Roche E. Single cell-derived clones from human adipose stem cells present different immunomodulatory properties. Clin Exp Immunol. 2014; 176:255-65.
13. Hao H, Liu J, Shen J, Zhao Y, Liu H, Hou Q, Tong C, Ti D, Dong L, Cheng Y, Mu Y, Liu J, Fu X, Han W. Multiple intravenous infusions of bone marrow mesenchymal stem cells reverse hyperglycemia in experimental type 2 diabetes rats. Biochem Biophys Res Commun. 2013; 436:418-23.
14. Liu X, Zheng P, Wang X, Dai G, Cheng H, Zhang Z, Hua R, Niu X, Shi J, An Y. A preliminary evaluation of efficacy and safety of Wharton's jelly mesenchymal stem cell transplantation in patients with type 2 diabetes mellitus. Stem Cell Res Ther. 2014; 5:57.
15. Hussien NI, Ebrahim N, Mohammed OM, Sabry D. Combination of Obestatin and Bone Marrow Mesenchymal Stem Cells Prevents Aggravation of Endocrine Pancreatic Damage in Type II Diabetic Rats. Int J Stem Cells. 2017; 10:129-43.
16. Tasev D, Koolwijk P, van Hinsbergh VW. Therapeutic Potential of Human-Derived Endothelial Colony-Forming Cells in Animal Models. Tissue Eng Part B Rev. 2016; 22:371-82.
17. Banno K, Yoder MC. Tissue regeneration using endothelial colony-forming cells: promising cells for vascular repair. Pediatr Res. 2018; 83:283-90.
18. Langford-Smith AWW, Hasan A, Weston R, Edwards N, Jones AM, Boulton AJM, Bowling FL, Rashid ST, Wilkinson FL, Alexander MY. Diabetic endothelial colony forming cells have the potential for restoration with glycomimetics. Sci Rep. 2019; 9:2309.
19. Reed MJ, Meszaros K, Entes LJ, Claypool MD, Pinkett JG, Gadbois TM, Reaven GM. A new rat model of type 2 diabetes: the fat-fed, streptozotocin-treated rat. Metabolism. 2000; 49:1390-4.
20. Mena HA, Zubiry PR, Dizier B, Schattner M, Boisson-Vidal C, Negrotto S. Acidic preconditioning of endothelial colony-forming cells (ECFC) promote vasculogenesis under proinflammatory and high glucose conditions in *vitro* and in *vivo*. Stem Cell Res Ther. 2018; 9:120.
21. Huang SP, Hsu CC, Chang SC, Wang CH, Deng SC, Dai NT, Chen TM, Chan JY, Chen SG, Huang SM. Adipose-derived stem cells seeded on acellular dermal matrix grafts enhance wound healing in a murine model of a full-thickness defect. Ann Plast Surg. 2012; 69:656-62.
22. Hu J, Fu Z, Chen Y, Tang N, Wang L, Wang F, Sun R, Yan S. Effects of autologous adipose-derived stem cell infusion on type 2 diabetic rats. Endocr J. 2015; 62:339-52.
23. Ho JH, Ma WH, Tseng TC, Chen YF, Chen MH, Lee OK. Isolation and characterization of multi-potent stem cells from human orbital fat tissues. Tissue Eng Part A. 2011; 17:255-66.
24. Williamson KA, Hamilton A, Reynolds JA, Sipos P, Crocker I, Stringer SE, Alexander YM. Age-related impairment of endothelial progenitor cell migration correlates with structural alterations of heparan sulfate proteoglycans. Aging Cell. 2013; 12:139-47.
25. Mahmoud AM, Wilkinson FL, Jones AM, Wilkinson JA, Romero M, Duarte J, Alexander MY. A novel role for small molecule glycomimetics in the protection against lipid-induced endothelial dysfunction: Involvement of Akt/eNOS and Nrf2/ARE signaling. Biochim Biophys Acta Gen Subj. 2017; 1861:3311-22.
26. Ingram DA, Mead LE, Tanaka H, Meade V, Fenoglio A, Mortell K, Pollok K, Ferkowicz MJ, Gilley D, Yoder MC. Identification of a novel hierarchy of endothelial progenitor cells using human peripheral and umbilical cord blood. Blood. 2004; 104:2752-60.
27. Kojić Damjanov S, Đerić M, Eremić Kojić N. Glycated hemoglobin A1c as a modern biochemical marker of glucose regulation. Med Pregl. 2014; 67:339-44.
28. Yin Q, Ma Y, Hong Y, Hou X, Chen J, Shen C, Sun M, Shang Y, Dong S, Zeng Z, Pei JJ, Liu X. Lycopene attenuates insulin signaling deficits, oxidative stress, neuroinflammation, and cognitive impairment in fructose-drinking insulin resistant rats. Neuropharmacology. 2014; 86:389-96.
29. El-Akabawy G and El-Kholy W. Neuroprotective effect of ginger in the brain of streprozotocin-induced diabetic rats. Ann Anat. 2014; 169: 119- 28.
30. El Agaty SM. Cardioprotective effect of vitamin D2 on isoproterenol-induced myocardial infarction in diabetic rats. Archives of Physiology and Biochemistry. 2019; 125:210-19.
31. Kiernan JA. Histological and histochemical methods: Theory and practice. 5th ed, Scion Publishing, Banbury, UK 2015; pp. 111-62.
32. Crisan M, Yap S, Casteilla L, Chen CW, Corselli M, Park TS, Andriolo G, Sun B, Zheng B, Zhang L, Norotte C, Teng PN, Traas J, Schugar R, Deasy BM, Badylak S, Buhring HJ, Giacobino JP, Lazzari L, Huard J, Péault B. A perivascular origin for mesenchymal stem cells in multiple human organs. Cell Stem Cell. 2008; 3:301-13.

33. Sweeney MD, Ayyadurai S, Zlokovic BV. Pericytes of the neurovascular unit: key functions and signaling pathways. Nat Neurosci. 2016; 19:771-83.

34. Seymour PA. Sox9: a master regulator of the pancreatic program. Rev Diabet Stud. 2014; 11:51-83.

35. Rezanejad H, Ouziel-Yahalom L, Keyzer CA, Sullivan BA, Hollister-Lock J, Li WC, Guo L, Deng S, Lei J, Markmann J, Bonner-Weir S. Heterogeneity of SOX9 and HNF1β in Pancreatic Ducts Is Dynamic. Stem Cell Reports. 2018; 10:725-38.

36. Suvarna K, Layton C, Bancroft J. Immunohistochemical techniques and Transmission electron microscopy In: Bancroft's Theory and practice of Histological Techniques, 7th ed, Churchill Livingstone Elsevier, Oxford. 2013. pp. 381-426- and 492-538.

37. Dykstra MJ, Reuss LE. Staining methods for ultra thins. In: Biological electron microscopy, theory, techniques and troubleshooting. 2nd ed, Kluwer Academic Publishers/Plenum Publishers. 2003. pp.175-96.

38. Sorour H, Selim M, Almoselhy L, Gouda S. Ameliorative Effect of Watermelon rind ingestion on the Pancreas of Diabetic Female Albino Rat (Histological, immunohistochemical and morphometric study). Egyptian Journal of Histology 2019; 42: 10-22.

39. Sani UM. Phytochemical Screening and Antidiabetic Effects of Extracts of the Seeds of Citrullus lanatus in Alloxaninduced Diabetic Albino Mice. J App Pharm Sci. 2015; 5: 51- 4.

40. Sena CM, Pereira AM, Seiça R. Endothelial dysfunction - a major mediator of diabetic vascular disease. Biochim Biophys Acta. 2013; 1832:2216-31.

41. Fadini GP, Albiero M, Bonora BM, Avogaro A. Angiogenic Abnormalities in Diabetes Mellitus: Mechanistic and Clinical Aspects. J Clin Endocrinol Metab. 2019; 104:5431-44.

42. Kang H, Yang C, Ahn H, Kang E, Hong E, Jeung. Effects of xenoestrogens on streptozotocin-induced diabetic mice. J Physiol Pharmacol. 2014; 65:273–82.

43. Song MY, Bae UJ, Lee BH, Kwon KB, Seo EA, Park SJ, Kim MS, Song HJ, Kwon KS, Park JW, Ryu DG, Park BH. Nardostachys jatamansi extract protects against cytokine- induced beta-cell damage and streptozotocin-induced diabetes. World J Gastroenterol. 2010; 16:3249-57.

44. Fraulob JC, Ogg-Diamantino R, Fernandes-Santos C, Aguila MB, Mandarim-de-Lacerda CA. A mouse model of metabolic syndrome: insulin resistance, fatty liver and non-alcoholic fatty pancreas disease (NAFPD) in C57BL/6mice fed a high fat diet. J Clin Biochem Nutr. 2010; 46:212-23.

45. Halban PA, Polonsky KS, Bowden DW, Hawkins MA, Ling C, Mather KJ, Powers AC, Rhodes CJ, Sussel L, Weir GC. β-cell failure in type 2 diabetes: postulated mechanisms and prospects for prevention and treatment. J Clin Endocrinol Metab. 2014; 99:1983-92.

46. Abdelmeguid NE, Fakhoury R, Kamal SM, AlWafai RJ. Effect of Nigella sativa L. and thymoquinone on streptozotocin induced cellular damage in pancreatic islets of rats. Asian J Cell Biol. 2011; 6:1–21.

47. Staels W, Heremans Y, Heimberg H, and De Leu N VEGF-A and blood vessels: a beta cell perspective. Diabetologia. 2019; 62: 1961-68.

48. Wang B, Zhang X, Liu M, Li Y, Zhang J, Li A, Zhang H, Xiu R. Insulin protects against type 1 diabetes mellitus-induced ultrastructural abnormalities of pancreatic islet microcirculation. Microscopy (Oxf). 2020; 69:381–90.

49. Almaça J, Weitz J, Rodriguez-Diaz R, Pereira E, Caicedo A. The Pericyte of the Pancreatic Islet Regulates Capillary Diameter and Local Blood Flow. Cell Metab. 2018; 27:630–44.

50. Shah P, Lueschen N, Ardestani A, Oberholzer J, Olerud J, Carlsson PO, Maedler K. Angiopoetin-2 signals do not mediate the hypervascularization of islets in type 2 diabetes. PLoS One. 2016; 11: e0161834. 86.

51. Dai C, Brissova M, Reinert RB, Nyman L, Liu EH, Thompson C, Shostak A, Shiota M, Takahashi T, Powers AC. Pancreatic islet vasculature adapts to insulin resistance through dilation and not angiogenesis. Diabetes.2013; 62:4144–53.

52. Shawky LM, Morsi AA, El Bana E, Hanafy SM. The Biological Impacts of Sitagliptin on the Pancreas of a Rat Model of Type 2 Diabetes Mellitus: Drug Interactions with Metformin. Biology (Basel). 2019; 9:6.

53. Armulik A, Genove G, Betsholtz C. Pericytes: developmental, physiological, and pathological perspectives, problems, and promises. Dev Cell. 2011; 21:193–215.

54. Spears E, Serafimidis I, Powers AC, Gavalas A. Debates in Pancreatic Beta Cell Biology: Proliferation Versus Progenitor Differentiation and Transdifferentiation in Restoring β Cell Mass. Front Endocrinol (Lausanne). 2021; 12:722250.

55. Wang M, Song L, Strange C, Dong X, Wang H. Therapeutic effects of adipose stem cells from diabetic mice for the treatment of type 2 diabetes. Mol Ther. 2018; 26:1921–30.

56. Dave SD, Vanikar AV, Trivedi HL. In-*vitro* generation of human adipose tissue derived insulin secreting cells: up-regulation of Pax-6, Ipf-1 and Isl-1. Cytotechnology. 2014; 66:299–307.

57. Cao M, Pan Q, Dong H, Yuan X, Li Y, Sun Z, Dong X, Wang H. Adipose-derived mesenchymal stem cells improve glucose homeostasis in high-fat diet-induced obese mice. Stem Cell Res Ther. 2015; 6:208.

58. Cannella V, Piccione G, Altomare R, Marino A, Di Marco P, Russotto L, Di Bella S, Purpari G, Gucciardi F, Cassata G, Damiano G, Palumbo VD, Santoro A, Russo Lacerna C, Lo Monte AI, Guercio A. Differentiation and characterization of rat adipose tissue mesenchymal stem cells into endothelial-like cells. Anat Histol Embryol. 2018; 47:11-20.

59. Mendel TA, Clabough EB, Kao DS, Demidova-Rice TN, Durham JT, Zotter BC, Seaman SA, Cronk SM, Rakoczy EP, Katz AJ, Herman IM, Peirce SM, Yates PA. Pericytes derived from adipose-derived stem cells protect against retinal vasculopathy. PLoS One. 2013;8: e65691.

60. Lynn FC, Smith SB, Wilson ME, Yang KY, Nekrep N, German MS. Sox9 coordinates a transcriptional network in pancreatic progenitor cells. Proc Natl Acad Sci U S A. 2007; 104:10500-5.

61. Li WC, Rukstalis JM, Nishimura W, *et al*. Activation of pancreatic-duct-derived progenitor cells during pancreas regeneration in adult rats. J Cell Sci. 2010; 123:2792–802.

62. Qi Y, Ma J, Li S, Liu W. Applicability of adipose-derived mesenchymal stem cells in treatment of patients with type diabetes. Stem Cell Res Ther. 2019; 10:274.

63. Kang KT, Lin RZ, Kuppermann D, Melero-Martin JM, Bischoff J. Endothelial colony forming cells and mesenchymal progenitor cells form blood vessels and increase blood flow in ischemic muscle. Sci Rep. 2017; 7:770.

64. Lin R-Z, Hatch A, Antontse VG *et al*. Microfluidic capture of endothelial colony-forming cells from human adult peripheral blood: Phenotypic and functional validation in *vivo*. Tissue Eng Part C Methods .2015; 21:274–83.

65. Souidi N, Stolk M, Rudeck J, Strunk D, Schallmoser K, Volk HD, Seifert M. Stromal Cells Act as Guardians for Endothelial Progenitors by Reducing Their Immunogenicity After Co-Transplantation. Stem Cells. 2017; 35:1233-45.

66. Narayanan S, Loganathan G, Dhanasekaran M, Tucker W, Patel A, Subhashree V, *et al*. Intra-islet endothelial cell and beta-cell crosstalk: implication for islet cell transplantation. World J Transplant. 2017; 7:117–28.

67. Lin HM, Lee JH, Yadav H, Kamaraju AK, Liu E, Zhigang D, Vieira A, Kim SJ, Collins H, Matschinsky F, Harlan DM, Roberts AB, Rane SG. Transforming growth factor-beta/Smad3 signaling regulates insulin gene transcription and pancreatic islet beta-cell function. J Biol Chem. 2009; 284:12246-57.

68. Alvarez-Perez JC, Rosa TC, Casinelli GP, Valle SR, Lakshmipathi J, Rosselot C, *et al*. Hepatocyte growth factor ameliorates hyperglycemia and corrects beta-cell mass in IRS2-deficient mice. Molecular Endocrinol (Baltimore, Md). 2014; 28:2038–48.

69. Yu CG, Zhang N, Yuan SS, Ma Y, Yang LY, Feng YM, Zhao D. Endothelial Progenitor Cells in Diabetic Microvascular Complications: Friends or Foes? Stem Cells Int, 2016; 2016:1803989.

70. Loibl M, Binder A, Herrmann M, Duttenhoefer F, Richards RG, Nerlich M, Alini M, Verrier S. Direct cell-cell contact between mesenchymal stem cells and endothelial progenitor cells induces a pericyte-like phenotype in *vitro*. Biomed Res Int. 2014; 2014:395781.

71. Armulik A, Abramsson A, Betsholtz C. Endothelial/pericyte interactions. Circ Res. 2005; 97:512-23.

72. Díaz-Flores L, Gutiérrez R, Madrid JF, Varela H, Valladares F, Acosta E, Martín-Vasallo P, Díaz-Flores L Jr. Pericytes. Morphofunction, interactions and pathology in a quiescent and activated mesenchymal cell niche. Histol Histopathol. 2009; 24: 909-69.

73. Chen J, Luo Y, Hui H, Cai T, Huang H, Yang F, Feng J, Zhang J, Yan X. CD146 coordinates brain endothelial cell-pericyte communication for blood-brain barrier development. Proc Natl Acad Sci U S A. 2017;114: E7622-E7631.

74. Houtz J, Borden P, Ceasrine A, Minichiello L, Kuruvilla R. Neurotrophin Signaling Is Required for Glucose-Induced Insulin Secretion. Dev Cell. 2016; 39:329–45.

75. O'Neill CL, McLoughlin KJ, Chambers SEJ, Guduric-Fuchs J, Stitt AW, Medina RJ. The Vasoreparative Potential of Endothelial Colony Forming Cells: A Journey Through Pre-clinical Studies. Front Med (Lausanne). 2018; 5:273.

76. Liu Y, Teoh SH, Chong MS, Lee ES, Mattar CN, Randhawa NK, Zhang ZY, Medina RJ, Kamm RD, Fisk NM, Choolani M, Chan JK. Vasculogenic and osteogenesis-enhancing potential of human umbilical cord blood endothelial colony-forming cells. Stem Cells 2012; 30:1911–24.

77. Lin R-Z, Moreno-Luna R, Li D, Jaminet S-C, Greene AK, Melero-Martin JM. Human endothelial colony-forming cells serve as trophic mediators for mesenchymal stem cell engraftment via paracrine signaling. Proc Natl Acad Sci U S A. 2014; 111:10137–42.

78. Waldenström A, Gennebäck N, Hellman U, Ronquist G. Cardiomyocyte microvesicles contain DNA/RNA and convey biological messages to target cells. PLoS One. 2012;7: e34653.

79. Zhang M, Lin Q, Qi T, Wang T, Chen CC, Riggs AD, Zeng D. Growth factors and medium hyperglycemia induce Sox9+ ductal cell differentiation into β cells in mice with reversal of diabetes. Proc Natl Acad Sci U S A. 2016; 113:650-5.

الملخص العربى

التأثيرات التفاعلية للخلايا المكونة للمستعمرات البطانية مع الخلايا الجذعية الدهنية الوسيطة علي البنكرياس في نموذج الجرذ السكري من النوع الثاني: دراسة هستولوجية

مروة محمد يسرى وإيمان عباس فرج

قسم علم الأنسجة ـ كلية الطب ـ جامعة القاهرة

الخلفية: ظهرت الخلايا الجذعية الدهنية الوسيطة كعلاج واعد لمرض السكري من النوع الثاني. وبالرغم من ذلك فربما يكون إعطاء الخلايا الجذعية الدهنية الوسيطة لمرة واحدة غير كافٍ لإحداث تأثيرات مستمرة مضادة لمرض السكري. تشارك الخلايا المكونة للمستعمرات البطانية في العديد من الوظائف البيولوجية مثل التوازن الوعائي ، وتخليق الأوعية الدموية الجديدة ، وتجديد الأنسجة.

الهدف من العمل: تقييم ومقارنة التأثير التجديدى للخلايا الجذعية الدهنية الوسيطة على مرض السكري المحدث من النوع الثاني في مراحل زمنية مختلفة و التأثير المحتمل عند العلاج بها مع الخلايا المكونة للمستعمرات البطانية.

المواد وطرق البحث: تم استخدام أربعة جرذان من إجمالي ستين من الذكور البالغين من الجرذان البيضاء لإعداد الخلايا الجذعية الدهنية الوسيطة والخلايا المكونة للمستعمرات البطانية وعلمت ب PKH٢٦. تم تقسيم الجرذان إلى أربع مجموعات رئيسية: المجموعة الأولي (الضابطة) ، والمجموعة الثانية (مرض السكري من النوع الثاني) التي تلقت نظامًا غذائيًا عالي الدهون لمدة خمسة أسابيع ثم تلقت حقنة واحدة داخل الغشاء البريتوني من STZ (٤٠ ملجم/ كجم) وأكملت النظامَ الغذائيَ عالي الدهون لمدة أسبوع . المجموعة الثالثة (المعالجة بالخلايا الجذعية الدهنية الوسيطة) الجرذان المصابة بالسكري والتي تلقت الخلايا الجذعية الدهنية الوسيطة ، والمجموعة الرابعة (المعالجة بالخلايا الجذعية الدهنية الوسيطة والخلايا المكونة للمستعمرات البطانية) الجرذان المصابة بالسكري والتي تلقت الخلايا الجذعية الدهنية الوسيطة والخلايا المكونة للمستعمرات البطانية. تم التضحية بجرذ واحد من المجموعتين الثالثة والرابعة والمقابل لهم من المجموعة الضابطة بعد اسبوع واحد من زرع الخلايا لتقييم وصول الخلايا لأنسجة البنكرياس. وتم التضحية بالجرذان المتبقية بعد أسبوعين وستة أسابيع. تم إجراء التحاليل الكيميائية الحيوية والدراسات الهستولوجية التي اشتملت علي صبغتي الهيماتوكسيلين والإيوسين ، والصبغة الهستوكيميائية المناعية ضد الأنسولين و SOX٩ و CD ١٤٦ و caspase-٣ ، والميكرسكوب الالكتروني، وأتبع ذلك بالقياسات المترية الشكلية والتحليل الإحصائي.

النتائج: أظهرت جرذان مرض السكري من النوع الثاني اختلال كيميائي حيوي ونسيجي في خلايا بيتا والأوعية الدموية بجزر لانجرهانز مع ظهور طبقات عديدة في النسيج الطلائي بالقنوات البنكرياسية. أظهرت الجرذان التي عولجت بـالخلايا الجذعية الدهنية الوسيطة فقط أوعولجت بها مع الخلايا المكونة للمستعمرات البطانية تحسنًا في استجابة الأنسولين وتوازن الجلوكوزوخصائص نسيجية طبيعية تقريبًا بعد أسبوعين. تراجع التحسن الكيميائي الحيوي والنسيجي بعد ستة أسابيع في الجرذان المعالجة بالخلايا الجذعية الدهنية الوسيطة. على العكس من ذلك ، فقد امتدت التأثيرات المضادة للسكري عند العلاج بالخلايا المكونة للمستعمرات البطانية مع الخلايا الجذعية الدهنية الوسيطة.

الاستنتاج: عزز وأطال العلاج بالخلايا المكونة للمستعمرات البطانية مع الخلايا الجذعية الدهنية الوسيطة من تأثيرها المضاد علي مرض السكري من النوع الثاني من خلال تجديد خلايا جزر لانجرهانز وتعزيز الأوعية الدموية لجزر لانجرهانز ، وربما عن طريق تمايز النسيج الطلائي بالقنوات.